Available online at www.sciencedirect.com

ScienceDirect

Energy Procedia 148 (2018) 591–598

Energy Procedia

www.elsevier.com/locate/procedia

73rd Conference of the Italian Thermal Machines Engineering Association (ATI 2018), 12-14 September 2018, Pisa, Italy

Numerical analyses of a high pressure sooting flame with multiphysics approach

Simone Paccati[a,*], Davide Bertini[a], Stefano Puggelli[a], Lorenzo Mazzei[a], Antonio Andreini[a], Bruno Facchini[a]

[a]*Department of Industrial Engineering, University of Florence, Via di S. Marta, 3, Firenze 50139, Italy*

Abstract

The development of a new standard for soot emissions proposed by ICAO-CAEP to reduce the environmental impact of civil aviation is moving increasingly research effort on the investigation of sooting flames. Formation and oxidation of the particulate matter are strongly affected by gas temperature, requiring an accurate prediction of the flow field from a numerical point of view. On the other hand, the temperature distribution within the combustor is modified by radiation, which depends on the soot concentration, leading to a very challenging coupled problem.

In this work, a series of sensitivity analyses in RANS context are performed on soot, radiation and heat transfer modelling to assess their impact on the prediction of soot emission, gas temperature as well as wall heat fluxes distribution in the context of a high pressure sooting flame which is representative of a RQL combustor. These results are employed to set up a CHT (*Conjugate Heat Transfer*) simulation, using the multiphysics THERM3D procedure in a loosely-coupled manner where reactive CFD, radiation and heat conduction calculations are computed sequentially with a separate solver in a dedicated framework. These sensitivities can provide useful information for the numerical setup in high-fidelity simulations, as Scale Resolving Simulations.

Keywords: Gas turbine; Combustion; Swirl flame; Ethylene; Soot; Radiation; CFD; RANS; FGM.

The reduction of chemical pollutants is still one of the main targets in the design of aero-engines. Therefore, continuous efforts have been devoted to the development of low emission combustors, such as Rich-Quench-Lean (RQL) technology and lean combustors, in order to respect the increasingly stringent regulations, especially in terms of soot production. These carcinogenic particles are the results of complex chemical processes which are strongly coupled with temperature distribution within the combustor, depending on mixing, on radiative heat transfer and on soot volume fraction itself and so making soot prediction a very challenging task.

*Corresponding author. Tel.: 39-055-275-8771.
E-mail address: simone.paccati@unifi.it

1876-6102
10.1016/j.egypro.2018.08.146

Considering the intrinsic difficulties and the costs in performing experimental campaigns at engine operating conditions, numerical simulations have become an essential tool for improving the design of combustion systems and for achieving reliable predictions of pollutant emissions. In this context, all complex phenomena which characterize reactive flows, such as combustion and turbulent transport and mixing, must be properly modeled.

The production of soot particles entails a negative effect on climate change and human health, as well as a reduction in the efficiency of the combustion devices, increasing heat loads due to thermal radiation. Therefore, multiphysics simulations such as CHT calculations are necessary to evaluate the impact of such emission on temperature distribution within the combustion chambers and to achieve a realible prediction of wall temperatures.

In this work, a series of numerical analyses is computed in a RANS context on DLR ethylene-air model aero engine combustor where both the geometry and the operating conditions are fully representative of a typical RQL combustor. In addition, a wide range of experimental measurements is available for gas and wall temperatures and soot mass concentration. These sensitivities represent a preliminary stage in order to assess a multiphysics simulation with THERM3D method, employing three loosely-coupled simulations for fluid, solid and radiation to evaluate wall temperatures with less computational time compared to a directly coupled solution of the reacting mixture with radiation and heat conduction by means of typical CHT approach [1].

Nomenclature

P Power [kW]
Q Volume flow rate [slm]
SN Swirl Number [-]

Acronysm
CFD Computational Fluid Dynamics
HTC Heat Transfer Coefficient
RANS Reynolds Averaged Navier Stokes

Greek
ϕ Equivalence ratio [-]

Subscripts
c central
r ring

1. Description of the methodology (THERM3D)

The multiphysics simulation involving both fluid and solid domains was performed exploiting the THERM3D procedure in order to optimize the computational resources. It belongs to the class of loosely-coupled approaches, that are characterized by a dedicated simulation for one or more physics and the coupling is recovered by ad-hoc boundary conditions at the interface between two different domains [1]. THERM3D solves in a sequential manner the convection, conduction and radiation steady-state problems, following the scheme reported in Figure 1.

The interaction among the simulations is accomplished through the exchange of data. Gas temperature, pressure and species fields are passed from the flow field solver to the radiation one. Source/sink and wall heat fluxes provided by the radiative computation are sent respectively to fluid and solid solvers. Wall heat fluxes coming from radiation and convection are used in the solid simulation, which returns to the others the metal temperature distribution. Convective wall heat fluxes are applied as a convection boundary condition, that is a particular case of the more stable Robin boundary condition. Concerning radiation, a black-body model is employed. Consequently, the computation of radiative gas temperature is required in order to set the radiative heat fluxes.

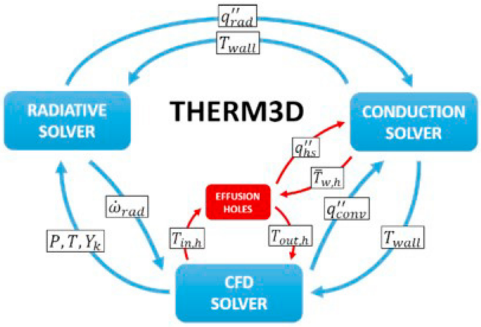

Fig. 1. Schematic representation of the THERM3D methodology [citazione

The sequential loop shown in Figure 1 is repeated until the convergence of the procedure, evaluated in terms of mean metal temperature variation between the last two iteration, is satisfied.

2. Experimental test case

The investigated test case is the DLR-FIRST combustor, experimentally investigated by Geigle et al. [5, 7] at the German Aerospace Center, for which a rich dataset of qualitative and quantitative experimental measurements are available for several operating conditions. The rig presents a square section of 68*x*68 mm^2 and is 120 *mm* high, surrounded by a stainless steel pressure housing. Quartz windows serve as combustor and housing walls in order to provide optical access to the internal reactive flow, as shown in Figure 2.

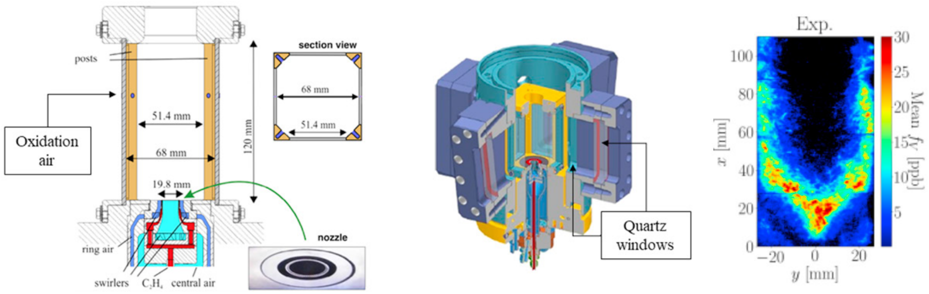

Fig. 2. Design of burner combustion chamber and optical module of pressure housing and soot volume fraction experimental map (adapted from [5, 7])

The injector consists of three concentric nozzles with a dual radial swirler configuration, generating a recirculation and leading to a highly turbulent region in the first part of the combustor. Primary air is supplied through both the central nozzle, passing a radial swirler which consists of 8 vanes (the swirl number is $SN = 0.82$) and an annular nozzle, passing a radial swirler composed of 11 vanes ($SN = 0.78$). Secondary air jets can be supplied through additional ducts which are located in the combustion chamber at a height of 80 *mm*, leading to a quench region and soot oxidation. The fuel is ethylene and it is injected through straight channels between air channels. For more information regarding the rig and the investigated operating conditions, the reader is addressed to [5]. In Table 1, the conditions of the considered operating point are reported.

Experimental measurements include gas temperature using Coherent Anti-Stokes Raman Spectroscopy (CARS) [6], time averaged soot distributions and instantaneous soot volume fraction maps [5].

Table 1. Considered operating point

Quantity	Value
Operating pressure [bar]	3
ϕ [-]	1.2
$P_{primary}$ [kW]	32.2
$Q_{air,c}$ [slm]	140.8
$Q_{air,r}$ [slm]	328.5
Q_{fuel} [slm]	39.3
Q_{oxi} [slm]	187.4

3. Numerical setup

The commercial code ANSYS Fluent v17.1 was employed to compute all simulations using a RANS approach. Therefore, the realizable k-ε [11] model was adopted in order to take into account turbulence effects. As shown in Figure 3, the employed computational domain includes the combustion chamber and the two radial swirlers, whereas also quartz windows are considered in THERM3D calculation.

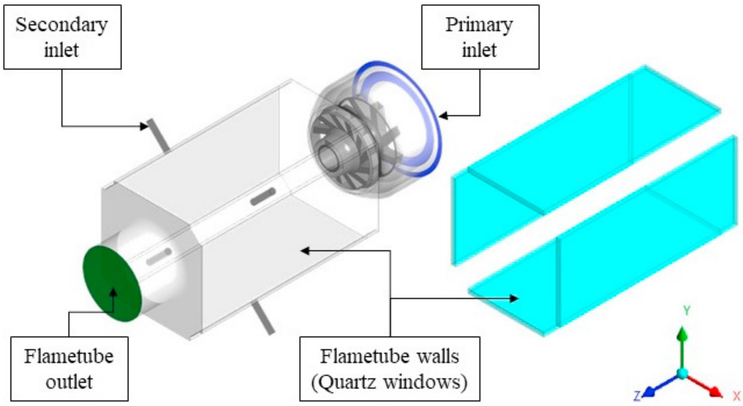

Fig. 3. Flametube and solid computational domains

For all simulations, a tetrahedral mesh of 14M elements with 3 prismatic layers close to the wall was employed for the gas phase simulation whereas heat conduction calculation within solid framework was performed in a hexahedral mesh of 600k elements, as shown in Figure 4. Instead, the radiative solver of the THERM3D simulation was supplied with a coarser tetrahedral mesh of 2.6M elements, as shown in Figure 4.

Regarding boundary conditions, top-hat profiles were imposed for velocity, temperature, mixture fraction and progress variable at inlets, whereas a static pressure was adopted at flametube outlet, according to data reported in Table 2. Smooth and no-slip conditions for velocity were considered for all walls while only quartz windows were treated as transparent to radiation. Whereas a uniform temperature of 900 K was adopted at the hot side of gas-solid interface for flametube calculations according to [3], a constant temperature (313 K) and HTC (121 W/m^2K) value were applied on the cold side of the quartz windows for THERM3D simulation, according to [10]

As far as combustion modelling is concerned, the Flamelet Generated Manifold (FGM) was adopted to describe the reactive flow behavior and the flame characteristics [12], parametrizing the chemical state and reaction progress space only as function of two control variables, the mixture fraction and a progress variable. The chemical kinetics were described employing Wang and Laskin mechanism developed for ethylene/air combustion [13] and so considering 75 species and 529 reactions, since the flame speed, the temperature and the flame structure but also the gaseous intermediate species such as acetylene and OH are correctly reproduced by this mechanism [4]. Flamelet equations

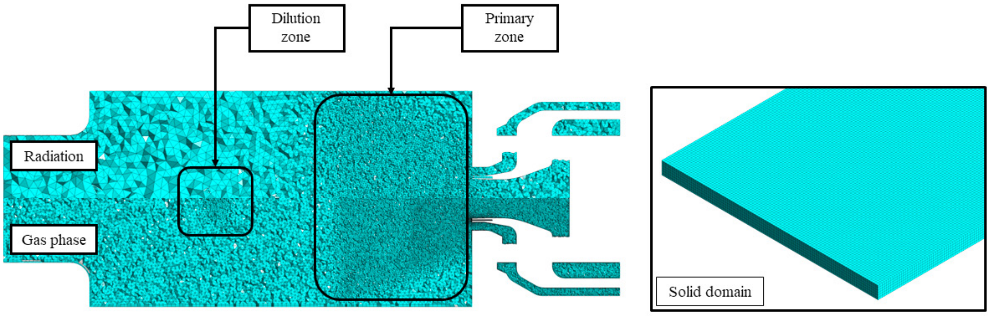

Fig. 4. Computational grid of fluid and solid domains

have been solved using the dedicated solver integrated in ANSYS Fluent, generating a set of $64x64$ non-premixed flamelets. Laminar quantities of the generated manifold are then integrated in the pre-processing stage using a beta-Probability Density Function (β-PDF) for both mixture fraction and progress variable.

In order to take into account soot formation within the combustor, two different models were considered: One-Step and Moss-Brookes models. The One-Step model exploits a single transport equation for the soot mass fraction [8]:

$$\frac{\delta(\rho Y_{soot})}{\delta t} + \nabla \cdot \left(\rho \vec{v} Y_{soot}\right) = \nabla \cdot \left(\frac{\mu_t}{\sigma_{nuc}} \nabla Y_{soot}\right) + R_{soot} \tag{1}$$

where R_{soot} is the net rate of soot generation related to the balance of soot formation and soot combustion.

Instead, two additional transport equations for radical nuclei concentration and soot mass fraction are solved according to Moss-Brooks approach [2]:

$$\frac{\delta(\rho b^*_{nuc})}{\delta t} + \nabla \cdot \left(\rho \vec{v} b^*_{nuc}\right) = \nabla \cdot \left(\frac{\mu_t}{\sigma_{nuc}} \nabla b^*_{nuc}\right) + \frac{1}{N_{norm}}\frac{dN}{dt} \tag{2}$$

$$\frac{\delta(\rho Y_{soot})}{\delta t} + \nabla \cdot \left(\rho \vec{v} Y_{soot}\right) = \nabla \cdot \left(\frac{\mu_t}{\sigma_{nuc}} \nabla Y_{soot}\right) + \frac{dM}{dt} \tag{3}$$

where M is soot mass concentration and N is soot particle number density. It is important to specify that the source term for soot mass concentration dM/dt takes into account different mechanisms of nucleation (source), surface growth (source) and oxidation (sink), whereas the instantaneous production rate of soot particles dN/dt considers the nucleation from the gas phase (source) and the coagulation in the free molecular regime (sink). The source terms of the considered transport equations show a strong non linear temperature dependence, making soot formation highly sensitive to spatial evolution of the flow.

The Radiative Transfer Equation (RTE) is solved employing Discrete Ordinate (DO) model [9], using two different setup in terms of angular discretization ($4x4, 8x8$) and pixelation ($3x3, 6x6$). As far as THERM3D simulation is concerned, radiative calculation is computed in a frozen gas phase solution with the coarser mesh to balance accuracy and CPU efforts, leading to a decrease of the computational cost of the entire simulation.

Here, a table is reported to summarize the computed simulations whose results are discussed in the following of this work.

4. Results and discussion

Results of the simulated operating condition are here highlighted. First of all, a comparison between the solutions of the sensitivities is reported in terms of temperature and soot volume fraction fields, evaluating also the significant impact of radiative phenomena on soot emission when radiation is not computed. Then, the result of THERM3D simulation is considered, focusing the attention on the computed wall temperatures.

Table 2. Computed simulation

Case	Simulation type	Turbulence model	Radiation model/discretization	Soot model
1	Flametube (isothermal condition)	k-ϵ	No computed	Moss-Brookes
2	Flametube (isothermal condition)	k-ϵ	DO (4x4/3x3)	Moss-Brookes
3	Flametube (isothermal condition)	k-ϵ	DO (8x8/6x6)	Moss-Brookes
4	Flametube (adiabatic walls)	k-ϵ	DO (4x4/3x3)	Moss-Brookes
5	Flametube (isothermal condition)	k-ϵ	DO (4x4/3x3)	One-Step model
6	THERM3D	k-ϵ	DO (4x4/3x3)	Moss-Brookes

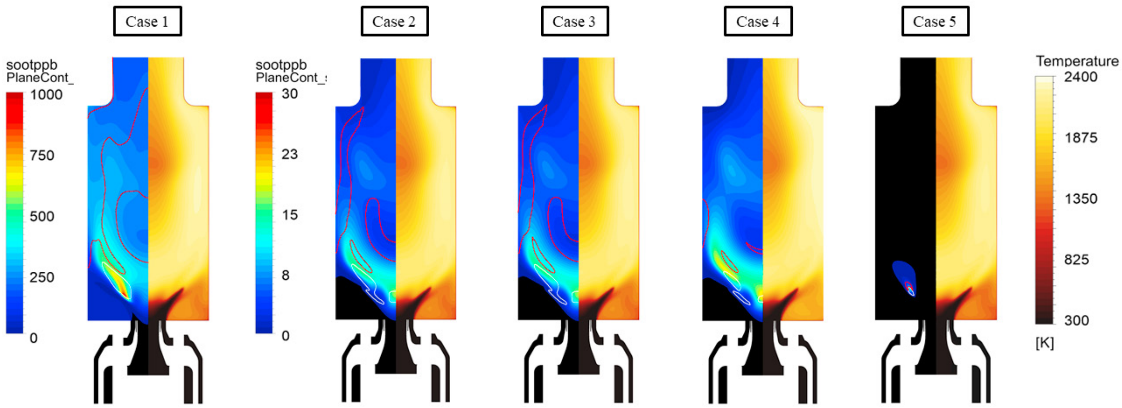

Fig. 5. Computed temperature and soot volume fraction distributions

Figure 5 shows computed temperature and soot volume fraction distributions in combustor mid plane. The typical features of RQL technology can be observed with a high temperature primary region characterized by hot gas recirculation and with a low temperature dilution zone where secondary oxidation air is injected.

From a first qualitative examination, comparable temperature fields are predicted by simulations where the k-ϵ model is employed and radiative phenomena are taken into account. Considering case 2 as the baseline simulation, no differencies can be appreciated compared to case 3 whereas higher temperatures can be observed next to the windows due to the adiabatic conditions in case 4. Slight differencies can be also noted in case 5, due to the different computed soot distribution, as shown below, and in case 1 where the absence of heat dispersion related to radiative emissions towards the cold external environment leads to a temperature increase, especially close to the swirler outlet and to the quartz windows.

Considering soot production, the pollutant particles are primarly formed in the high temperature region close to the swirler and in the outer part of the recirculation zone with a peak on the centerline when radiation is taken into account. Then, they are trasported downstream close to the walls where dilution air causes soot oxidation. The white line is the iso-contour at 15% of soot mass source maximum value (related to soot formation) while the red line is the iso-contour at 15% of its minimum value (related to soot oxidation). As shown in case 1 radiative phenomena have a strong impact on soot emissions, determining an increase of two orders of magnitude of the peak values when radiative calculation is not computed, probably related to the strong non-linear dependence on temperature of the source terms of soot model equations. Instead, case 5 shows a global under-prediction with formation and oxidation limited to a small region next to the swirler outlet.

A deeper understanding of the effects of soot, radiation and wall boundary conditions on temperature distribution within the combustor can be appreciated in Figure 6 where temperature differences of each case are reported with respect to case 2. The left comparison shows the impact of radiation (left) and the influence of a different soot prediction (right), whereas the relevance of a proper wall temperature computation can be observed on the right side.

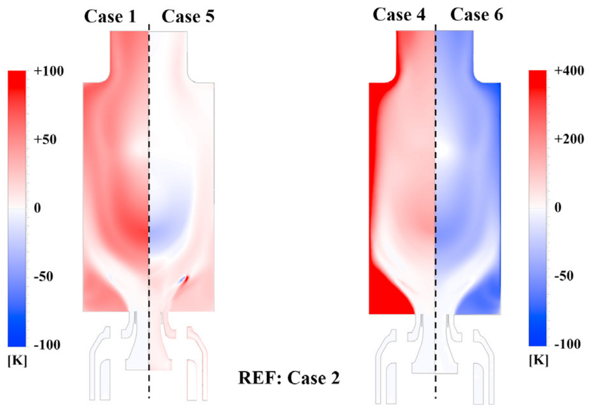

Fig. 6. Temperature differences of each case with respect to case 2

Figure 7 shows instead the results of THERM3D simulation, computed with case 2 settings since better matching with experimental data can be apprecieted as shown below. A general qualitative agreement with experimental map in terms of soot production is highlighted, pointing out the capabilities of Moss-Brookes model to predict the evolution of soot production processes.

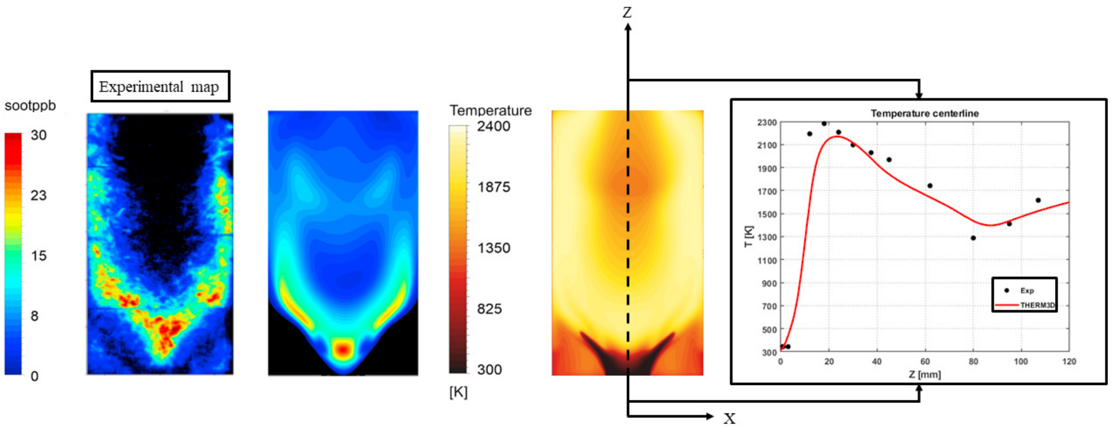

Fig. 7. Distribution on the mid plane and profiles along the centerline of the combustor in terms of temperature and soot volume fraction

Considering temperature profiles along the centerline of the combustion chamber, the comparison with experimental data highlights general good agreement. It is possible to note an under-prediction of about 60 K in the first part of the combustor, whereas an over-prediction of about 100 K occurs at 80 mm downstream of swirler outlet, probably related to the employed steady approach.

As far as wall temperatures are concerned, significant discrepancies can be observed from a quantitative comparison with measurements along the centerline. Figure 8 shows an underprediction of wall temperatures, especially in the primary zone. This is probably related to the inaccuracy of RANS approach in the prediction of turbulence effects which higly affects the mixing and the combustion processes, leading to an underestimation of flow radial spreading and so resulting in a less impact of hot flows on flametube walls.

5. Conclusions

This work presents a series of numerical analyses on the DLR ethylene-air model aero engine combustor with a RANS approach. The results are employed to set up a multiphysics THERM3D simulation in order to predict wall

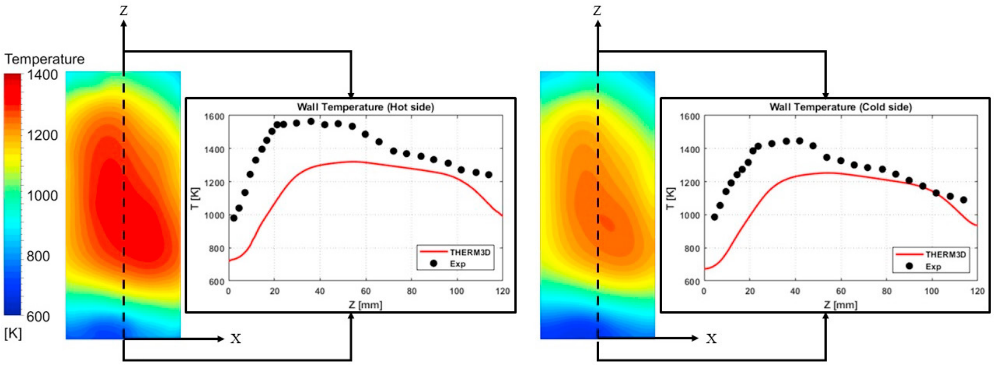

Fig. 8. Quartz windows temperatures

temperatures within the investigated combustor. As shown in the preliminary sensitivity stage, radiative heat transfer is strongly coupled with soot production, affecting both temperature and soot volume fraction fields. Depending on the employed models and the imposed boundary conditions, different levels and distributions of soot formation and oxidation occur. However, THERM3D method allows to achieve a reliable prediction of temperature and soot volume fraction distributions in the gas domain, whereas discrepancies with experimental data can be observed in terms of wall temperatures, propably due to the employed steady approach which fails in the computation of the flow radial spreading.

References

[1] Bertini, D., Mazzei, L., Puggelli, S., Andreini, A., Facchini, B., Bellocci, L., Santoriello, A., 2018. Numerical and experimental investigation on an effusion-cooled lean burn aeronautical combustor: Temperature profiles and emissions, in: Proceedings of GT2018 ASME TURBO EXPO 2018: Power for Land, Sea & Air.

[2] Brookes, S., Moss, J., 1999. Predictions of soot and thermal radiation properties in confined turbulent jet diffusion flames. Combustion and Flame 116, 486–503.

[3] Eberle, C., Gerlinger, P., Geigle, K.P., Aigner, M., 2015. Numerical investigation of transient soot evolution processes in an aero-engine model combustor. Combustion Science and Technology 187, 1841–1866.

[4] Franzelli, B., Riber, E., Cuenot, B., Ihme, M., 2015. Numerical modeling of soot production in aero-engine combustors using large eddy simulations, in: ASME Turbo Expo 2015: Turbine Technical Conference and Exposition, American Society of Mechanical Engineers. pp. V04BT04A049–V04BT04A049.

[5] Geigle, K.P., Hadef, R., Meier, W., 2014. Soot formation and flame characterization of an aero-engine model combustor burning ethylene at elevated pressure. Journal of Engineering for Gas Turbines and Power 136, 021505.

[6] Geigle, K.P., Köhler, M., O'Loughlin, W., Meier, W., 2015a. Investigation of soot formation in pressurized swirl flames by laser measurements of temperature, flame structures and soot concentrations. Proceedings of the Combustion Institute 35, 3373–3380.

[7] Geigle, K.P., O'Loughlin, W., Hadef, R., Meier, W., 2015b. Visualization of soot inception in turbulent pressurized flames by simultaneous measurement of laser-induced fluorescence of polycyclic aromatic hydrocarbons and laser-induced incandescence, and correlation to oh distributions. Applied Physics B 119, 717–730.

[8] Khan, I.M., Greeves, G., 1974. A method for calculating the formation and combustion of soot in diesel engines. Heat transfer in flames , 389–404.

[9] Murthy, J., Mathur, S., 1998. Finite volume method for radiative heat transfer using unstructured meshes. Journal of thermophysics and heat transfer 12, 313–321.

[10] Rodrigues, P., Gicquel, O., Darabiha, N., Geigle, K.P., Vicquelin, R., 2018. Assessment of external heat transfer modeling of a laboratory-scale combustor inside a pressure-housing environment, in: Proceedings of GT2018 ASME TURBO EXPO 2018: Turbomachinery Technical Conference & Exposition.

[11] Shih, T.H., Liou, W.W., Shabbir, A., Yang, Z., Zhu, J., 1995. A new k-ϵ eddy viscosity model for high reynolds number turbulent flows. Computers & Fluids 24, 227–238.

[12] Van Oijen, J.A., 2002. Flamelet-generated manifolds: development and application to premixed laminar flames. Technische Universiteit Eindhoven Eindhoven.

[13] Wang, H., Laskin, A., 1998. A comprehensive kinetic model of ethylene and acetylene oxidation at high temperatures. Progress Report for an AFOSR New World Vista Program .